Toward an Understanding of the Anion Effect in CpRu-Based Diels−Alder Catalysts via PGSE-NMR Measurements

P. G. Anil Kumar and P. S. Pregosin*

Laboratory of Inorganic Chemistry, ETHZ, Hönggerberg, CH-8093 Zürich, Switzerland

M. Vallet, G. Bernardinelli, R. F. Jazzar, F. Viton, and E. P. Kündig*

Department of Organic Chemistry, University of Geneva, 30 Quai Ernest Ansermet, CH-1211 Geneva 4, Switzerland

Received June 16, 2004

The rate dependence of the [Ru(η^5-C_5H_5)(BIPHOP-F)(acetone)][Y]-catalyzed Diels−Alder reaction of cyclopentadiene with methacrolein on the anion, Y, is shown to be due to selective ion pairing. Pulsed gradient spin−echo (PGSE) diffusion measurements on the model Cp and indenyl complexes [Ru(η^5-C_5H_5)(CH_2=CH-CN)(BIPHOP-F)][Y], Y = BF_4 and BArF, and [Ru(η^5-C_9H_7)(CH_2=CH-CN)(BIPHOP-F)][Y], Y = BF_4 and BArF, respectively, combined with ^{1}H−^{19}F HOESY NMR data can be used to understand how the ion pairing for the BF_4 anion differs relative to that of the BArF anion. Solid-state structures for [Ru(η^5-C_5H_5)(CH_2=CH-CN)(BIPHOP-F)][BF_4] and [Ru(η^5-C_5H_5)(CH_2=CH-CN)(BIPHOP-F)][BArF] are reported and support the NMR solution data. The model carbonyl complexes [Ru(η^5-C_5H_5)(BIPHOP-F)-(CO)][Y], **8** (Y = BF_4, SbF_6, and BArF) have been synthesized. The IR CO stretching frequencies for **8** showed little variation with anion, thereby proving that the anions do not affect the Lewis acidity of the salts.

Introduction

Although cationic transition metal complexes are important catalysts and reagents in organic synthesis,[1−5] the role of the anion is not often investigated in these reactions. This despite the fact that anion/cation interactions can dramatically affect solubility of the catalyst, accelerate or decelerate reactions, improve reaction selectivity, or even change its course.[6] Anions such as BF_4^-, PF_6^-, and SbF_6^- are often thought to be noncoordinating; however, recent evidence shows that even these anions are capable of coordination to the cation, either directly or via hydrogen bonding.[7] A number of reports show that the presence of the counterion $BArF^-$ (tetrakis(3,5-bis(trifluoromethyl)phenyl)borate) accelerates selected reactions when compared to PF_6^- or BF_4^-.[6a,8,9] Moreover, cations can assist in the hydrolysis of anions, e.g., PF_6^-.[10] Thus, while it is well known that the counteranion (e.g., BF_4^-, PF_6^-, SbF_6^-, and $BArF^-$) influences not only the solubility of the salt but also its reactivity, the precise role of the anion is not often established.

Recently, it was found that the rate of the enantioselective Diels−Alder reaction of cyclopentadiene with methacrolein, catalyzed by [Ru(η^5-C_5H_5)(BIPHOP-F)-(acetone)][Y] (**1**), depends on the nature of the anion, Y (Scheme 1).[2] A similar, though less pronounced, trend was found for the indenyl analogue [Ru(η^5-C_9H_7)-(BIPHOP-F)(acetone)][Y] (**2**).[11]

(1) (a) Genêt, J. P. *Acros Org. Acta* **1995**, *1*, 4. (b) Wiles, J. A.; Bergens, S. H.; Young, V. G. *J. Am. Chem. Soc.* **1997**, *119*, 2940. (c) Ohkuma, T.; Ishii, D.; Takeno, H.; Noyori, R. *J. Am. Chem. Soc.* **2000**, *122*, 6510.

(2) (a) Kündig, E. P.; Saudan, C. M.; Bernardinelli, G. *Angew. Chem., Int. Ed.* **1999**, *38*, 1220. (b) Davenport, A. J.; Davies, D. L.; Fawcett, J.; Garratt, S. A.; Russell, D. R. *J. Chem. Soc., Dalton Trans.* **2000**, 4432. (c) Faller, J. W.; Lavoie, A. R.; Grimmond, B. J. *Organometallics* **2002**, *21*, 1662. (d) Viton, F.; Bernardinelli, G.; Kündig, E. P. *J. Am. Chem. Soc.* **2002**, *124*, 4968. (e) Carmona, D.; Lamata, M. P.; Viguri, F.; Rodriguez, R.; Oro, L. A.; Balana, A. I.; Lahoz, F. J.; Tejero, T.; Merino, P.; Franco, S.; Montesa, I. *J. Am. Chem. Soc.* **2004**, *126*, 2716.

(3) Pregosin, P. S.; Salzmann, R. *Coord. Chem. Rev.* **1996**, *155*, 35.

(4) (a) Trost, B. M.; Van Vranken, D. L. *Chem. Rev.* **1996**, *96*, 395. (b) Trost, B. M.; Toste, F. D. *J. Am. Chem. Soc.* **2002**, *124*, 5025. (c) Trost, B. M.; Shen, H. C.; Schulz, T.; Koradin, C.; Schirok, H. *Org. Lett.* **2003**, *5*, 4149. (d) Trost, B. M.; Rudd, M. T. *Org. Lett.* **2003**, *5*, 4599.

(5) Fagnou, K.; Lautens, M. *Angew. Chem., Int. Ed.* **2002**, *41*, 26.

(6) (a) Evans, D. A.; Murry, J. A.; von Matt, P.; Norcross, R. D.; Miller, S. J. *Angew. Chem., Int. Ed. Engl.* **1995**, *34*, 798. (b) Trost, B. M.; Bunt, R. C. *J. Am. Chem. Soc.* **1998**, *120*, 70. (c) Macchioni, A.; Bellachioma, G.; Cardaci, G.; Travaglia, M.; Zuccaccia, C.; Milani, B.; Corso, G.; Zangrando, E.; Mestroni, G.; Carfagna, C.; Formica, M. *Organometallics* **1999**, *18*, 3061. (d) Ludwig, M.; Stroemberg, S.; Svensson, M.; Akermark, B. *Organometallics* **1999**, *18*, 970. (e) Rifat, A.; Patmore, N. J.; Mahon, M. F.; Weller, A. S. *Organometallics* **2002**, *21*, 2856. (f) Takenaka, N.; Huang, Y.; Rawal, V. H. *Tetrahedron* **2002**, *58*, 8299.

(7) (a) Romeo, R.; Nastasi, N.; Scolaro, L. M.; Plutino, M. R.; Albinati, A.; Macchioni, A. *Inorg. Chem.* **1998**, *37*, 5460. (b) Song, J.-S.; Szalda, D. J.; Bullock, R. M. *Organometallics* **2001**, *20*, 3337.

(8) Pfaltz, A.; Blankenstein, J.; Hilgraf, R.; Hormann, E.; McIntyre, S.; Menges, F.; Schonleber, M.; Smidt, S. P.; Wustenberg, B.; Zimmermann, N. *Adv. Synth. Catal.* **2003**, *345*, 33.

(9) (a) Carmona, D.; Elipe, S.; Lahoz, F. J.; Oro, L. A.; Cativiela, C.; Pilar Lopez-Ram de Viu, M.; Pilar Lamata, M.; Vega, C.; Viguri, F. *Chem. Commun.* **1997**, 2351. (b) Kündig, E. P.; Saudan, C. M.; Viton, F. *Adv. Synth. Catal.* **2001**, *343*, 51.

(10) (a) Connelly, N. G.; Einig, T.; Herbosa, G. G.; Hopkins, P. M.; Mealli, C.; Orpen, A. G.; Rosair, G. M.; Viguri, F. *J. Chem. Soc., Dalton Trans.* **1994**, 2025. (b) Kitagawa, S.; Kondo, M.; Kawata, S.; Wada, S.; Maekawa, M.; Munakata, M. *Inorg. Chem.* **1995**, *34*, 1455. (c) Drago, D.; Pregosin, P. S. *Organometallics* **2002**, *21*, 1208.

(11) Kündig, E. P.; Saudan, C. M.; Alezra, V.; Viton, F.; Bernardinelli, G. *Angew. Chem., Int. Ed.* **2001**, *40*, 4481.

10.1021/om049559o CCC: $27.50
Publication on Web 10/08/2004

Scheme 1

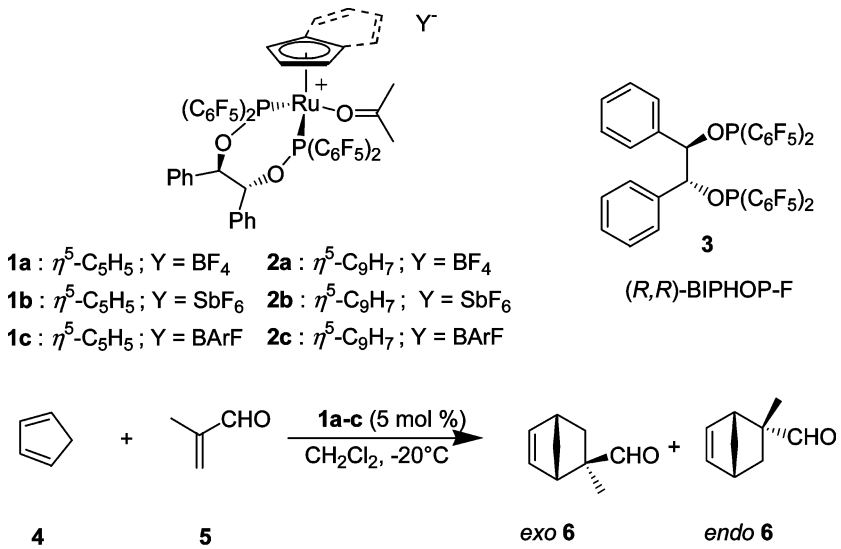

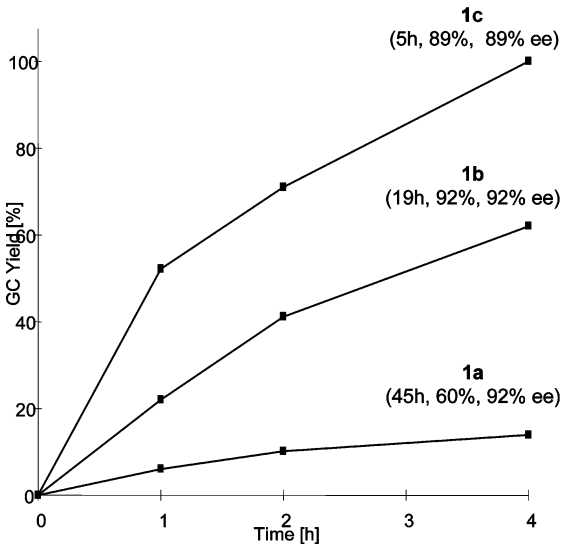

The reactions are fastest with the counterion $BArF^-$, and rates decreased in the order $BArF^- > SbF_6^- > PF_6^- > BF_4^-$. The X-ray crystal structure[2a] of [Ru(η^5-C_5H_5)-(BIPHOP-F)(methacrolein)][SbF_6] showed a close proximity of the anion/cation with distances between F and the H atoms of the aldehyde and Cp ligand below the sum of van der Waals radii. Preliminary HOESY NMR studies of the corresponding PF_6^- complex showed these interactions to exist also in solution. In this paper we wish to report the results of more detailed studies carried out in order to delineate the origins of the anion effect in this family of compounds. The primary technique used for this investigation is pulsed gradient spin–echo (PGSE) NMR.[12]

PGSE NMR diffusion studies provide information on the size of species in solution and on intermolecular or interionic interactions.[12] Measuring translational properties of the molecules, this technique is directly responsive to molecular size and shape and has found widespread application.[13–16] As diffusion methodology readily recognizes ion pairing,[16] we turned to this technique to analyze the Ru-cation/anion interactions. When a large transition metal cation containing a bulky

(12) (a) Stilbs, P. *Prog. NMR Spectrosc.* **1987**, *19*, 1. (b) Price, W. S. *Ann. Rep. NMR Spectrosc.* **1996**, *32*, 51. (c) Price, W. S. *Concepts Magn. Reson.* **1997**, *9*, 299. (d) Price, W. S. *Concepts Magn. Reson.* **1998**, *10*, 197. (e) Price, W. S.; Stilbs, P.; Soderman, O. *J. Magn. Reson.* **2003**, *160*, 139.

(13) (a) Mo, H. P.; Pochapsky, T. C. *J. Phys. Chem. B* **1997**, *101*, 4485. (b) Harris, R. K.; Kinnear, K. A.; Morris, G. A.; Stchedroff, M. J.; Samadi-Maybodi, A.; Azizi, N. *Chem. Commun.* **2001**, 2422. (c) Dvinskikh, S. V.; Furo, I.; Sandstroem, D.; Maliniak, A.; Zimmermann, H. *J. Magn. Reson.* **2001**, *153*, 83. (d) Deaton, K. R.; Feyen, E. A.; Nkulabi, H. J.; Morris, K. F. *Magn. Reson. Chem.* **2001**, *39*, 276. (e) Wan, Y.; Angleson, J. K.; Kutateladze, A. G. *J. Am. Chem. Soc.* **2002**, *124*, 5610. (f) Schlorer, N. E.; Cabrita, E. J.; Berger, S. *Angew. Chem.* **2002**, *41*, 107.

(14) (a) Zuccaccia, D.; Sabatini, S.; Bellachioma, G.; Cardaci, G.; Clot, E.; Macchioni, A. *Inorg. Chem.* **2003**, *42*, 5465. (b) Stahl, N. G.; Zuccaccia, C.; Jensen, T. R.; Marks, T. J. *J. Am. Chem. Soc.* **2003**, *125*, 5256.

(15) (a) Beck, S.; Geyer, A.; Brintzinger, H.-H. *Chem. Commun.* **1999**, 2477. (b) Olenyuk, B.; Levin, M. D.; Whiteford, J. A.; Shield, J. E.; Stang, P. J. *J. Am. Chem. Soc.* **1999**, *121*, 10434. (c) Gorman, C. B.; Smith, J. C.; Hager, M. W.; Parkhurst, B. L.; Sierzputowska-Gracz, H.; Haney, C. A. *J. Am. Chem. Soc.* **1999**, *121*, 9958. (d) Stoop, R. M.; Bachmann, S.; Valentini, M.; Mezzetti, A. *Organometallics* **2000**, *19*, 4117. (e) Burini, A.; Fackler, J. P., Jr.; Galassi, R.; Macchioni, A.; Omary, M. A.; Rawashdeh-Omary, M. A.; Pietroni, B. R.; Sabatini, S.; Zuccaccia, C. *J. Am. Chem. Soc.* **2002**, *124*, 4570.

(16) (a) Martinez-Viviente, E.; Rueegger, H.; Pregosin, P. S.; Lopez-Serrano, J. *Organometallics* **2002**, *21*, 5841. (b) Pregosin, P. S.; Martinez-Viviente, E.; Kumar, P. G. A. *Dalton Trans.* **2003**, 4007. (c) Martinez-Viviente, E.; Pregosin, P. S. *Inorg. Chem.* **2003**, *42*, 2209. (d) Kumar, P. G. A.; Pregosin, P. S.; Goicoechea, J. M.; Whittlesey, M. K. *Organometallics* **2003**, *22*, 2956.

Scheme 2. Synthesis of [Ru(η^5-C_5H_5)(BIPHOP-F)(CO)][Y] Complexes

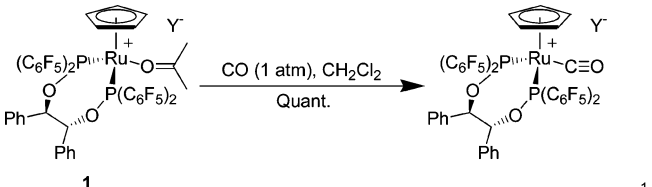

1

8a : Y = BF_4 : ν_{CO} = 2028 cm^{-1}
8b : Y = SbF_6 : ν_{CO} = 2029 cm^{-1}
8c : Y = BArF : ν_{CO} = 2033 cm^{-1}

chelating ligand, such as BIPHOP-F (**3**) or BINAP (**7**), forms strong ion pairs (or hydrogen bonds) with a smaller anion, e.g., BF_4^-, the diffusion constant (*D* value) for the latter is markedly reduced. Consequently, if one uses both ^{1}H and ^{19}F NMR methods to monitor the individual cation and anion *D* values (and more importantly, the changes in these), ion pairing can be explored in a direct fashion. We report here new PGSE diffusion, X-ray crystallographic, and preparative studies for a number of cationic half-sandwich complexes of ruthenium and suggest an explanation for the observed anion effect.

Results and Discussion

Infrared Measurements. The increase in the catalytic reactivity of the complexes upon going from BF_4^- to $BArF^-$ could possibly be attributed to an electronic contribution of the counteranion to the Lewis acidity of the transition metal center. To evaluate this hypothesis, we examined the IR carbonyl stretching frequencies of the complexes [Ru(η^5-C_5H_5)(BIPHOP-F)(CO)][Y] (Y = BF_4 **8a**, SbF_6 **8b**, and BArF **8c**). IR ν_{CO} shifts are very sensitive to the metal electron density, and they are generally taken as a reliable measure for the extent of π-back-donation in metal carbonyl complexes.[17]

The requisite carbonyl complexes, **8a**−**c**, were readily obtained in quantitative yield upon bubbling CO gas through a CH_2Cl_2 solution of the corresponding acetone complex[2] at room temperature. As shown in Scheme 2, the stretching frequencies showed little variation. If at all, the anion has only a very small influence on the withdrawing properties of the cation. Moreover, we have established that for the CpRu catalyst precursor **1b** the rate-determining step is not the Diels−Alder reaction but the product/adduct exchange. This follows from the observation that the reaction rate remains unchanged upon increasing 5-fold the amount of diene.[9b]

PGSE and ^{1}H−^{19}F HOESY Measurements. Prior to investigating the Ru-BIPHOP-F complexes, we established PGSE data for the closely related complexes [Ru(η^5-C_5H_5)(BINAP)(CH_3CN)][Y], **9** (see Scheme 3), derived from [Ru(η^5-C_5H_5)(BINAP)Cl], **10**. Very little diffusion data are known for η^5-C_5H_5 complexes, and a comparison of complexes differing in the nature of the chiral phosphorus ligand is valuable. In addition, the new complexes offered an interesting comparison with our previously measured [Ru(η^6-*p*-cymene)(BINAP)Cl]-[Y], **11**, complexes.[16d] The complexes **9** were prepared

Scheme 3

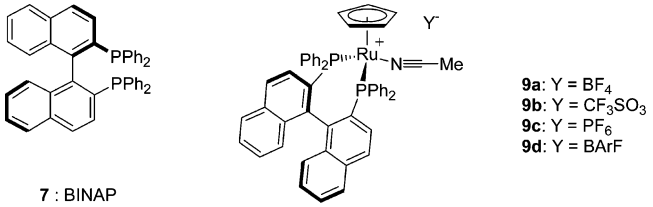

7 : BINAP

9a: Y = BF_4
9b: Y = CF_3SO_3
9c: Y = PF_6
9d: Y = BArF

Table 1. Diffusion Values[a] and Hydrodynamic Radii for 9a−d and 10

		CD_2Cl_2		$CDCl_3$		$(CD_3)_2CO$	
	compound	*D*	r_h (Å)	*D*	r_h (Å)	*D*	r_h (Å)
cation {^{1}H}	**9a**, BF_4	8.26	6.5	6.07	6.8	10.73	6.8
anion {^{19}F}		12.33	4.3	6.14	6.8	26.84	2.7
cation {^{1}H}	**9b**, CF_3SO_3	8.16	6.6	6.00	6.9	10.51	6.9
anion {^{19}F}		12.16	4.4	6.14	6.8	24.63	2.9
cation {^{1}H}	**9c**, PF_6	8.36	6.4	6.13	6.8	10.64	6.8
anion {^{19}F}		12.30	4.4	6.52	6.4	26.89	2.7
cation {^{1}H}	**9d**, BArF	7.76	6.9	4.78	8.6	10.31	7.0
anion {^{1}H}		7.93	6.8	4.97	8.5	11.47	6.3
neutral {^{1}H}	**10**	8.51	6.3	6.53	6.4		

[a] Measured at 400 MHz, 2 mM; *D* values, 10^{-10} m^2 s^{-1}.

by treating the known complex [Ru(η^5-C_5H_5)(PPh_3)$_2$Cl] with BINAP, **7**, followed by abstraction of the halide using a variety of silver salts in the presence of acetonitrile to afford the complexes [Ru(η^5-C_5H_5)(BINAP)(CH_3CN)][Y] (Y = BF_4 **9a**, CF_3SO_3 **9b**, PF_6 **9c**, and BArF **9d**). Table 1 shows the measured *D* values in chloroform, acetone, and dichloromethane together with the hydrodynamic radii, r_h, which were calculated using the Stokes−Einstein equation.

$$D = kT/6\pi\eta r_h \quad (1)$$

where k = Boltzmann constant, T = absolute temperature, η = viscosity, and r_h = hydrodynamic radius.

Data from the neutral complex [Ru(η^5-C_5H_5)(BINAP)-Cl] (**10**) have also been obtained and provide an indication as to the correct *D* value and hydrodynamic radius for this class (ca. 6.3−6.4 Å) in the absence of strong solvation and/or ion-pairing effects.

As we have now come to expect,[16] the chloroform data reveal tight ion pairing, i.e, close to equivalent translation rates for both cation and anion. Due to the ion pairing the calculated r_h values are larger in chloroform than, for example, dichloromethane, especially for the $BArF^-$ salt. The acetone r_h values for the cations are all on the large side. We have no obvious explanation for this, although we have observed this effect previously.[16b] Further, in acetone, the BF_4^-, $CF_3SO_3^-$, and PF_6^- all give relatively small r_h values, ca. 2.7−2.9 Å.

In dichloromethane, the r_h values for the BF_4^-, $CF_3SO_3^-$, and PF_6^- anions **9a**−**c**, respectively, are all relatively large and suggest a significant ion pairing. To support this idea, ^{1}H−^{19}F HOESY spectra in dichloromethane have been measured for the BF_4^-, $CF_3SO_3^-$, and $BArF^-$ salts. Figure 1 shows NOE contacts from the $CF_3SO_3^-$ anion to the bound acetonitrile, the η^5-C_5H_5 ligand, and some of the aromatic protons. The analogous BF_4^- spectrum shows the same contacts as the $CF_3SO_3^-$ anion; however, the $BArF^-$ anion shows no signals in the ^{1}H−^{19}F HOESY spectrum. The strong CH_3CN contact in dichloromethane suggests that the

(17) (a) Tolman, C. A. *J. Am. Chem. Soc.* **1970**, *92*, 2953. (b) Tolman, C. A. *Chem. Rev.* **1977**, *77*, 313. (c) Kündig, E. P.; Dupre, C.; Bourdin, B.; Cunningham, A., Jr.; Pons, D. *Helv. Chim. Acta* **1994**, *77*, 421.

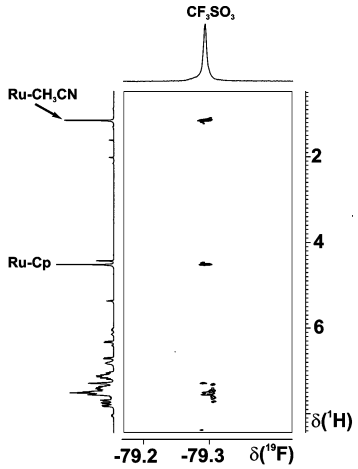

Figure 1. $^1H-^{19}F$ HOESY spectrum of complex [Ru(η^5-C_5H_5)(CH_3CN)(BINAP)][CF_3SO_3], **9b**. The small additional Cp resonance at ca. 4.4 ppm arises from the Cp signal for **18** (OTf) in which the BINAP is a 6e$^-$ donor (see Experimental Section).

Scheme 4. Variation of the Labile Ligand L in the Cationic Cp and Indenyl Ru Complexes

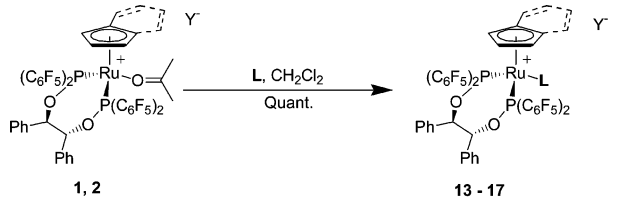

1, 2 13 - 17

13a : η^5-C_5H_5 ; L : Water ; Y = BF_4
13b : η^5-C_5H_5 ; L : Water ; Y = SbF_6
13c : η^5-C_5H_5 ; L : Water ; Y = BArF
14a : η^5-C_9H_7 ; L : Water ; Y = BF_4
14b : η^5-C_9H_7 ; L : Water ; Y = SbF_6
14c : η^5-C_9H_7 ; L : Water ; Y = BArF
***RR*-15a** : η^5-C_5H_5 ; L : Acrylonitrile ; Y = BF_4
***RR*-15b** : η^5-C_5H_5 ; L : Acrylonitrile ; Y = BArF
16a : η^5-C_9H_7 ; L : Acrylonitrile ; Y = BF_4
16b : η^5-C_9H_7 ; L : Acrylonitrile ; Y = BArF
17a : η^5-C_5H_5 ; L : Acetonitrile ; Y = BF_4
17b : η^5-C_5H_5 ; L : Acetonitrile ; Y = BArF

anion approaches the positive metal center via the bound nitrile.

The present diffusion data reveal that the Cp complexes **9** and the *p*-cymene complexes **11** behave similarly, but that, perhaps, the *p*-cymene complexes[16d] for Y = BF_4 and CF_3SO_3 possess slightly larger volumes (smaller *D* values) than the η^5-C_5H_5 complexes.

With this background we turned our attention to the BIPHOP-F complexes. Attempts to use the methacrolein complex [Ru(η^5-C_5H_5)(BIPHOP-F)($CH_2CH(Me)CHO$)][Y], **12**, met with difficulties because of the presence of small amounts of the aquo complex [Ru(η^5-C_5H_5)(BIPHOP-F)(H_2O)][Y], **13**. The same difficulty was encountered with the indenyl complexes where [Ru(η^5-C_9H_7)(BIPHOP-F)(H_2O)][Y], **14**, was present as an impurity. The catalytic system was closely mimicked through the synthesis of the acrylonitrile complexes [Ru(η^5-C_5H_5)(CH_2=CHCN)(BIPHOP-F)][Y], **15**, and [Ru(η^5-C_9H_7)(CH_2=CHCN)(BIPHOP-F)][Y], **16** (see Scheme 4). The complexes **15** and **16** containing the same anions were readily obtained in quantitative yield from the reaction of the corresponding acetone complexes with excess acrylonitrile in CH_2Cl_2 at room temperature.

Results from the ^1H and ^{19}F PGSE measurements for the model Ru-BIPHOP-F derivatives, [Ru(η^5-C_5H_5)(CH_2=CHCN)(BIPHOP-F)][Y], **15**, and [Ru(η^5-C_9H_7)(CH_2-CHCN)(BIPHOP-F)][Y], **16**, with Y = BF_4 and BArF, in dichloromethane and acetone are given in Table 2.

Table 2. Diffusion Values and Hydrodynamic Radii for 15a,b–17a,b[a]

		CD_2Cl_2		$(CD_3)_2CO$	
	compound	D	r_h (Å)	D	r_h (Å)
cation {^1H}	*RR*-**15a**, BF_4	7.84	6.8	9.72	7.5
anion {^{19}F}		9.67	5.5	27.36	2.6
cation {^1H}	*RR*-**15b**, BArF	7.28	7.4	9.44	7.7
anion {^1H}		7.84	6.8	11.85	6.1
cation {^1H}	**16a**, BF_4	7.80	6.9	9.17	7.9
anion {^{19}F}		9.79	5.5	24.45	3.0
cation {^1H}	**16b**, BArF	7.20	7.4	9.16	7.9
anion {^1H}		7.90	6.8	11.44	6.3
cation {^1H}	**17a**, BF_4	7.95	6.7	9.82	7.4
anion {^{19}F}		8.96	6.0	24.19	3.0
cation {^1H}	**17b**, BArF	7.39	7.2	9.58	7.6
anion {^1H}		7.99	6.7	11.85	6.1

[a] Measured at 400 MHz, 2 mM; *D* values, 10^{-10} m^2 s^{-1}.

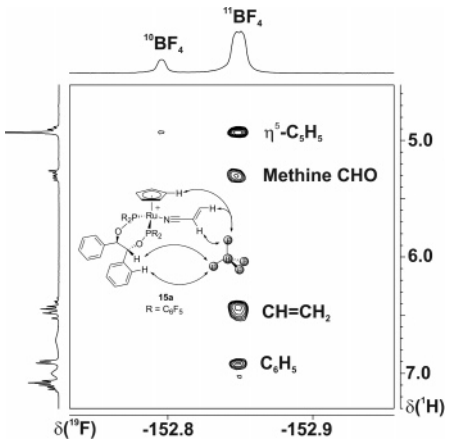

Figure 2. $^1H-^{19}F$ HOESY spectrum of complex [Ru(η^5-C_5H_5)(CH_2=CHCN)(BIPHOP–F)][BF_4], **15a**. Note that only one of the CHO backbone resonances, at ca. 5.3 ppm, shows a cross-peak and that there is selectivity to one of the phenyl rings. The second methine CHO signal appears to low frequency of the η^5-C_5H_5 resonance.

In dichloromethane solutions the calculated r_h values (5.5 Å) for the BF_4^- anion in both *RR*-**15a** and **16a** are clearly too large to arise from a simple solvate of BF_4^- and suggest surprisingly strong ion pairing. In solvents not promoting strong ion pairing, e.g., acetone or methanol, the r_h value for the BF_4^- anion is normally ca. 2.6–3.0 Å. The 5.5 Å value was the largest r_h we have yet found for this anion in this solvent. However, the cation r_h values for *RR*-**15a** and **16a**, ca. 6.8–6.9 Å, are reasonable enough. To further explore the observed solvent dependence of the ion pairing, the $^1H-^{19}F$ HOESY spectra of *RR*-**15a** and **16a** were measured. These spectra show selective contacts to one of the CHO backbone signals, the vinyl protons of the acrylonitrile, the η^5-ligand, and additional contacts to the *ortho* protons of one of the phenyl groups (see Figure 2). In the case of the BArF salts, in dichloromethane solution, *RR*-**15b** and **16b** both afford r_h values for the anion of 6.8 Å. These radii are close to what we find for the BINAP compound **9d** and other salts that we have reported.[16d] A typical r_h value for BArF salts in acetone or methanol is ca. 6.1–6.3 Å; therefore a 6.8 Å value is consistent with some interactions, but would not be considered as predominant ion pairing.

X-ray Studies on *RR*-15a and *RR*-15b. For both *RR*-**15a** and *RR*-**15b**, the above-mentioned NMR observations are in good agreement with the full molecular

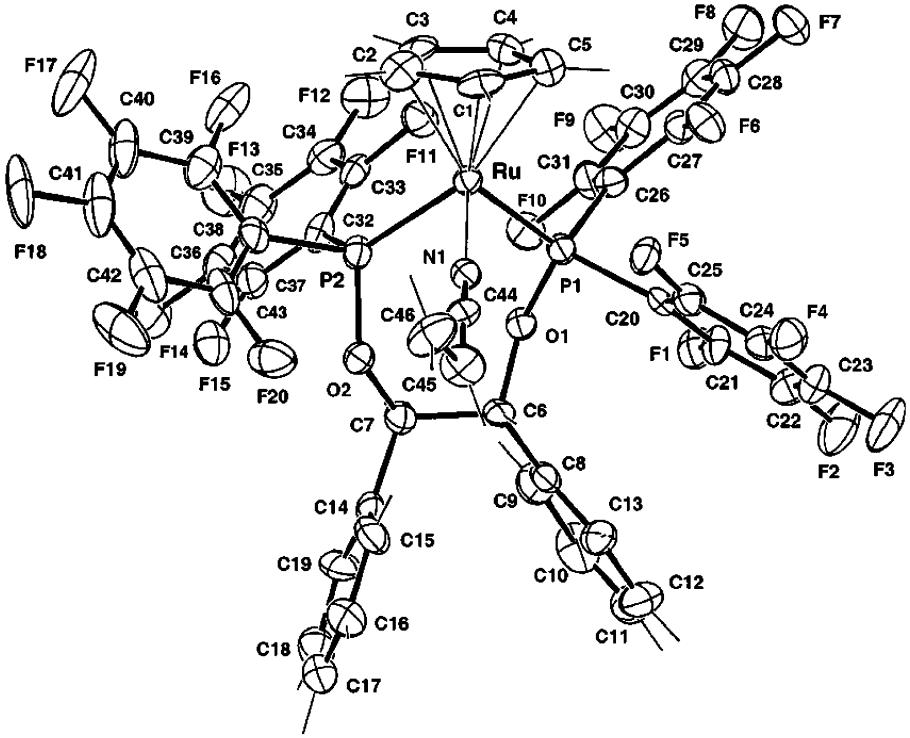

Figure 3. Perspective view of the cationic moiety of the crystal structure of $[Ru(C_{46}H_{20}NO_2F_{20}P_2)][BF_4]$, *RR*-**15a**, with atom numbering (the numbering scheme for *RR*-**15b** is identical). Ellipsoids are represented with 30% probability.

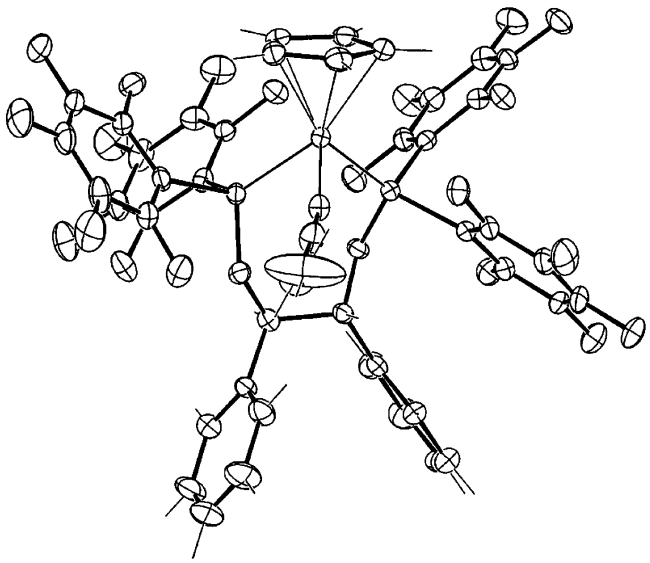

Figure 4. Perspective view of the cationic moiety of the crystal structure of $[Ru(C_{46}H_{20}NO_2P_2F_{20})][C_{32}H_{12}F_{24}B]$, *RR*-**15b** with atom numbering and showing the large displacement parameters affecting the terminal carbon atom (C46) of the acrylonitrile ligand. Ellipsoids are represented with 30% probability.

geometry of these complexes, which was elucidated by crystallographic measurements as shown in Figure 3 and Figure 4, respectively. Selected bond distances and bond angles are given in Table 3. Both *RR*-**15a** and *RR*-**15b** exhibit distorted piano-stool geometries with the coordinated acrylonitrile ligand embedded within the chiral pocket**.** In the case of *RR*-**15a** the asymmetric unit contains two complexes of the same absolute configuration, *RR*-**15a** and *RR*-**15a′**, which adopt almost identical conformations.

Table 3. Selected Geometrical Parameters for *RR*-15a and *RR*-15b

	RR-**15a**	*RR*-**15a′**	*RR*-**15b**
	Bond Lengths (Å)		
Ru(1)−P(1)	2.249(4)	2.258(4)	2.268(2)
Ru(1)−P(2)	2.260(3)	2.256(3)	2.257(2)
Ru(1)−N(1)	2.02(1)	2.04(1)	2.050(5)
Ru(1)−C(1)	2.23(2)	2.24(2)	2.234(7)
Ru(1)−C(2)	2.24(1)	2.20(2)	2.256(7)
Ru(1)−C(3)	2.18(1)	2.18(1)	2.248(7)
Ru(1)−C(4)	2.16(1)	2.17(1)	2.210(6)
Ru(1)−C(5)	2.25(1)	2.21(2)	2.218(6)
N(1)−C(44)	1.14(2)	1.11(2)	1.150(8)
C(44)−C(45)	1.45(2)	1.48(2)	1.42(1)
C(45)−C(46)	1.29(3)	1.30(3)	1.09(2)
Ru(1)−$Cp_{(mean\ plane)}$	1.867(1)	1.859(2)	1.880(1)
	Bond Angles (deg)		
P(1)−Ru(1)−P(2)	89.6(1)	90.3(1)	89.34(6)
P(1)−Ru(1)−N(1)	95.8(3)	94.8(3)	86.2(1)
P(2)−Ru(1)−N(1)	87.1(3)	85.9(3)	97.2(2)
Ru(1)−P(1)−O(1)	115.8(3)	116.9(3)	115.9(2)
Ru(1)−P(2)−O(2)	117.2(3)	117.9(4)	115.6(2)

The Ru−N bond lengths in *RR*-**15a** (2.02(1) and 2.04(1) Å) and *RR*-**15b** (2.050(5) Å) are in line with other Ru−NC−R complexes (e.g., 2.041 Å for $[Ru(\eta^5\text{-}C_5H_5)(CH_3CN)(PPh_3)_2][BF_4]$).[18] As observed previously in the case of $[Ru(\eta^5\text{-}C_5H_5)(BIPHOP\text{-}F)(CH_2{=}C(CH_3)CHO)][SbF_6]$,[2] the fluorine atoms of the BF_4 anions are involved in H···F interactions with both the hydrogen atoms of the Cp and acrylonitrile ligands (H···F distances smaller than 3.0 Å), thereby shielding the chiral binding site (see Table 4). Interestingly, one finds a single orientation of the acrylonitrile vinyl group with respect to the Cp ligand.

The solid-state structure of the $BArF^-$ complex *RR*-**15b** presents interesting differences relative to the BF_4^-

(18) Carreon, O. Y.; Leyva, M. A.; Fernandez-G., J. M.; Penicaud, A. *Acta Crystallogr., Sect. C: Cryst. Struct. Commun.* **1997**, *53*, 301.

Table 4. C-H···F Hydrogen Bond Interactions Involved between the Acrylonitrile and the Counterions

	C···F (Å)	H···F (Å)	C–H···F (deg)
RR-**15a**[a] (BF_4)			
C45–H45···F3c	3.32(2)	2.72	119
C45–H45···F4c	3.16(2)	2.59	117
C46 H462···F1d	3.13(2)	2.45	126
C46–H462···F4d	3.49(3)	2.59	154
RR-**15a′**[a] (BF_4)			
C45–H45···F1c[(i)b]	3.45(2)	2.70	134
C45–H45···F2c[(i)b]	3.21(2)	2.63	118
C46–H462···F2d[(ii)b]	3.44(2)	2.50	156
C46–H462···F4d[(ii)b]	3.30(3)	2.50	137
RR-**15b** (BArF)			
C45–H45···F4a[(iii)b]	3.41(1)	2.98	107
C46–H462···F8a[(iv)b]	3.59(2)	2.60	171

[a] The interactions with the other disordered fluorine atoms have been omitted for clarity. [b] Equivalent positions for the fluorine atoms: *(i)*: $x, y, z + 1$; *(ii)*: $1 - x, y - 1/2, 2 - z$; *(iii)*: $x + 1, y, z + 1$; *(iv)*: $2 - x, 1/2 + y, 1 - z$.

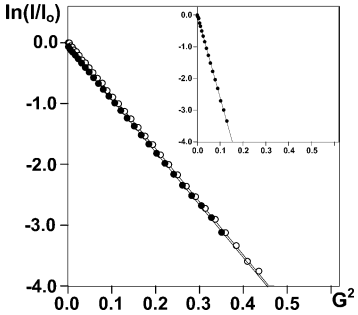

Figure 5. Diffusion data for the complex [Ru(η^5-C_5H_5)(CH_3-CN)(BIPHOP-F)][BF_4], **17a**, in dichloromethane. The white circles depict the translation of the cation, while the black ones are those for the anion. The inset shows the diffusion for the anion in acetone-d_6.

complex. Once again the anion is placed so that one finds relatively short contacts between the $BArF^-$ anion and both the Cp ring and the acrylonitrile ligand, via H···F interactions, but these are less numerous and weaker as shown in Table 4. The moderate interaction of the $BArF^-$ anion with the acrylonitrile results in more freedom for the vinyl moiety, as indicated by the large displacement parameters (see Figures 3 and 4) observed in the acrylonitrile fragment with respect to *RR*-**15a**. Although not directly related to the solution structure, this difference hints at the higher catalytic activity observed in the case of the $BArF^-$ anion.

Solution Studies on [Ru(η^5-C_5H_5)(CH_3CN)(BIPHOP-F)][BF_4], 17a. Returning to the solution data, the 5.5 Å r_h value observed in both *RR*-**15a** and **16a** was sufficiently unexpected for us to study the parent acetonitrile complex [Ru(η^5-C_5H_5)(CH_3CN)(BIPHOP-F)][BF_4], **17a** (see Table 2). In this case the r_h value for the BF_4^- anion in dichloromethane of 6.0 Å is now so large that ion pairing has to be invoked as a major contributor to the total structure (see Figure 5). The size of the cation remains unchanged, as attaching BF_4^- does not significantly change its volume. Once again, the $^1H-^{19}F$ HOESY (see Figure 6) confirms selective contacts. The selectivity concerns the CHO methine resonances, in that the resonance at δ 4.9 ppm does not show a contact, whereas that at δ 5.5 ppm does. The BArF analogue, **17b**, affords D and r_h values that are similar to those for **16**. We note that on the basis of

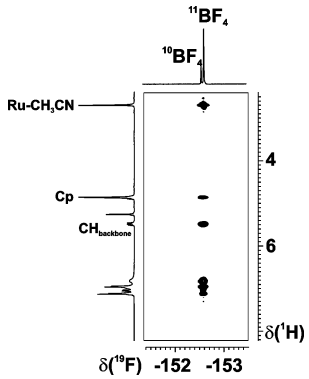

Figure 6. $^1H-^{19}F$ HOESY spectrum of the complex [Ru(η^5-C_5H_5)(CH_3CN)(BIPHOP-F)][BF_4], **17a**.

detailed $^1H-^{19}F$ HOESY results, Macchioni and coworkers[19] have recently suggested strong interionic contacts of the BF_4^- anion in a [Pt(alkene)(Me)(diimine)][BF_4] salt in dichloromethane. Consequently, this ion pairing appears to have some generality.

The aquo complexes [Ru(η^5-C_5H_5)(BIPHOP-F)(H_2O)][BF_4], **13a**, and [Ru(η^5-C_9H_7)(BIPHOP-F)(H_2O)][BF_4], **14a**, are observed when the acetone analogues, e.g., [Ru(η^5-C_5H_5)(acetone)(BIPHOP-F)][BF_4], **1a**, were dissolved in wet acetone-d_6.

For **13a**, the complexed water shows a two-proton resonance at ca. δ 3.5. Interestingly, the D values/r_h (Å) in dichloromethane for the BF_4^- anion (8.30/6.4 Å), the complexed water (7.86/6.8 Å), and the Ru cation (7.88/6.8 Å) are all similar. This is understandable since HOESY spectroscopy shows a strong NOE between the BF_4^- and the water signal, suggesting H-bonding as the source of this reduced BF_4^- translation. Phase-sensitive $^1H-^1H$ NOE studies show that the water signal is in slow exchange with free water, and we estimate the exchange rate, based on magnetization transfer studies, to be ca. 7 s^{-1} in CD_2Cl_2 and 20–30 s^{-1} in CD_3COCD_3. This observation is not relevant for the Diels–Alder chemistry since the reaction solvent is dry, and this brings us to a possible explanation for the BF_4^-/$BArF^-$ anion effect.

Comments and Conclusion. In the Diels–Alder reactions, catalyzed by the Ru-Lewis acids **1** and **2**, in dichloromethane, no significant difference in the values of product ee as a function of anion is observed. However, the reaction rates are quite different. This suggests that substrate/product coordination as a function of anion may be important. If the BF_4^- anion ion pairs strongly, it might well interfere with the complexation of the dienophile oxygen donor, slow the aldehyde exchange, or hinder the approach of the diene. Any of the above would be sufficient to slow the reaction. The $BArF^-$ anion is not so strongly ion paired, and HOESY and X-ray measurements reveal little or no contacts between the CF_3 groups (or *ortho* aryl protons) and the cation. The increased distance of this anion from the reactive site would provide a rationale for the higher turnover frequency of the catalyst. Clearly the PGSE/HOESY NMR combination provides a powerful methodology for recognizing the source of unexpected cation–anion interactions.

(19) Zuccaccia, C.; Macchioni, A.; Orabona, I.; Ruffo, F. *Organometallics* **1999**, *18*, 4367.

Table 5. Summary of Crystal Data, Intensity Measurement, and Structure Refinement for *RR*-15a and *RR*-15b

	RR-**15a**	*RR*-**15b**
formula	$[Ru(C_{46}H_{20}F_{20}NO_2P_2)]_2(BF_4)_2(CH_2Cl_2)$	$[Ru(C_{46}H_{20}F_{20}NO_2P_2)](C_{32}H_{12}F_{24}B)$
MW	2581.9	2024.9
cryst syst	monoclinic	monoclinic
space group	$P2_1$	$P2_1$
a (Å)	11.5543(7)	12.1877(8)
b (Å)	23.1672(9)	17.2400(8)
c (Å)	20.9274(15)	18.6316(13)
β (deg)	96.751(8)	96.268(8)
V (Å^3)	5563.0(6)	3891.4(4)
Z, Z'	2, 2	2, 1
D_{calc} (g cm^{-3})	1.541	1,728
cryst size (mm)	0.09 × 0.13 × 0.31	0.10 × 0.29 × 0.32
cryst color	yellow	yellow
radiation	Mo Kα	Mo Kα
μ (mm^{-1})	0.504	0.398
T_{min}, T_{max}	0.9208, 0.9563	0.9042, 0.9673
$((\sin\theta)/\lambda)_{max}$ (Å^{-1})	0.615	0.638
temperature (K)	200	200
no. measured reflns	64 413	54 465
no. indep reflns	21 032	16 910
no. obsd reflns	12 526	10 903
R_{int}	0.057	0.046
criterion for obsd	$\|F_o\| > 4\sigma(F_o)$	$\|F_o\| > 4\sigma(F_o)$
refinement (on F)	full-matrix	full-matrix
no. params	1462	1189
weighting scheme P[a]	0.00025	0.00015
Flack parameter, x	0.01(4)	−0.02(1)
max. Δ/σ	0.036	0.033
min. and max. $\Delta\rho$ (e Å^{-3})	−0.59, 0.93	−1.25, 0.55
S	1.94(2)	1.26(1)
R, R_w	0.045, 0.047	0.031, 0.030

[a] $w = 1/[\sigma^2(F_o) + P(F_o)^2]$.

Experimental Section

General Procedures. ^{1}H, ^{31}P, and ^{19}F spectra were recorded on Bruker Avance 250, 300, or 400 spectrometers. Chemical shifts are quoted in parts per million (ppm) downfield of tetramethylsilane. ^{31}P NMR chemical shifts were referenced externally to 85% H_3PO_4 (δ 0.0). ^{19}F NMR chemical shifts were referenced externally to $CFCl_3$ (δ 0.0). Coupling constants J are quoted in Hz. ^{13}C NMR and DEPT-135 spectra were recorded with a broad band probe. IR spectra were recorded on a Perkin-Elmer 1600 FT-IR spectrometer using a Golden Gate accessory. Elemental analysis was performed by the EA-Service of the Laboratory of Organic Chemistry (ETHZ). Mass-spectra were obtained by the MS-Service of the Laboratory of Organic Chemistry (ETHZ, MALDI, matrix 2,5-dihydroxybenzoic acid (DHB)). The exact mass measurement in TOF mode was obtained by electrospray using a quadrupole time-of-flight Q STAR XL (Applied Biosystems/MDS Sciex) mass spectrometer.

Unless otherwise stated, conventional (but not deuterated) solvents were purified, degassed, and dried by standard methods (distillation). $[Ru(\eta^5\text{-}C_5H_5)(CH_3CN)_3][PF_6]$ was prepared according to the literature.[20]

X-ray Crystal Structures. A summary of crystal data, intensity measurement, and structure refinement for *RR*-**15a** and *RR*-**15b** is reported in Table 5. Cell dimensions and intensities were measured at 200 K on a Stoe-IPDS diffractometer. Data were corrected for Lorentz and polarization effects and for absorption. The crystal structures were solved by direct methods using Sir-97.[21] All calculations were performed with XTAL system[22] and ORTEP[23] programs. Both independent molecules of the asymmetric unit of *RR*-**15a** are similar. CD spectra of both crystals used for the structure determination confirm the reported values below.

CCDC-240176 and CCDC-240177 contain the supplementary crystallographic data in cif format for *RR*-**15a** and *RR*-**15b**. These data can be obtained free of charge via www.ccdc.cam.ac.uk/conts/retrieving.html (or from the Cambridge Crystallographic Data Centre, 12 Union Road, Cambridge CB2 1EZ, UK; fax: (+ 44) 1223-336-033; or deposit@ccdc.cam.ac.uk).

Diffusion. All the measurements were performed on Bruker AVANCE spectrometers (300, 400, and 500 MHz) equipped with a microprocessor-controlled gradient unit and a multinuclear probe (normal or inverse) with an actively shielded Z-gradient coil. The shape of the gradient pulse was rectangular, their length was 1.75 ms, and its strength varied automatically in the course of the experiment. The time between midpoints of the gradients (Δ) was chosen as 167.75 ms. The measurements were carried out without sample spinning and in the absence of external airflow. The experiments were carried out at 299 K for our RT measurements, which were controlled by a digital BVT 3000 variable-temperature unit.

The diffusion values for the Cp and indenyl complexes are measured in the solvents indicated in the tables. The concentration of all the samples was maintained at 2 mM. The diffusion of the cation was measured using the ^{1}H signal from the Cp, indenyl, or hydrocarbon backbone, whereas the anion diffusion was obtained using the ^{19}F signal.

The error coefficients for the D values based on our experience is ±0.06.

The viscosities used in the Stokes−Einstein relation are those of pure solvents: CH_2Cl_2, 0.405; $CHCl_3$, 0.529; $(CH_3)_2CO$, 0.303.[24]

Synthesis. All reactions involving air-sensitive compounds were carried out in an atmosphere of purified nitrogen using an inert gas/vacuum double manifold and standard Schlenk or glovebox techniques.

Synthesis of RuCl(η^5-C_5H_5)(BINAP) (10). In a typical experiment, $RuCl(\eta^5\text{-}C_5H_5)(PPh_3)_2$ (866 mg, 1.20 mmol), BINAP (733 mg, 1.20 mmol), and 50 mL of toluene were placed in a Schlenk tube fitted with a magnetic stirrer. The mixture was then stirred at 120 °C for 5 days, during which time the formation of red crystals was observed. The precipitate was collected and washed twice with pentane and then dried, in vitro, to afford 670 mg (0.80 mmol, 68%) of pure product. Anal. Calcd for $C_{49}H_{37}ClP_2Ru$: C, 71.36; H, 4.61. Found: C, 71.40; H, 4.52. ^{1}H NMR (400 MHz, CD_2Cl_2): δ 7.89−7.82 (m, 2H, ArH), 7.60−7.44 (m, 6H, ArH), 7.38−7.22 (m, 11H, ArH), 7.15−7.05 (m, 3H, ArH), 7.01−6.88 (m, 4H, ArH), 6.80−6.74 (m, 2H, ArH), 6.65−6.59 (m, 2H, ArH), 6.38 (d, J = 9 Hz, 1H, ArH), 6.28 (d, J = 9 Hz, 1H, ArH), 4.22 (s, 5H, η^5-C_5H_5). ^{31}P{^{1}H} NMR (161.9 MHz, CD_2Cl_2): δ 54.4 (d, J_{PP} = 64 Hz), 44.8 (d, J_{PP} = 64 Hz). MS (MALDI): 789 (M^+ − Cl) (100).

Synthesis of [Ru(η^5-C_5H_5)(CH_3CN)(BINAP)][BF_4] (9a). In a typical experiment, a Schlenk tube was loaded with RuCl(η^5-C_5H_5)(BINAP) (119 mg, 0.15 mmol), $AgBF_4$ (28 mg, 0.15 mmol), and 3 mL of dry acetonitrile. The solution was then stirred in the dark overnight, after which time the solvent was evaporated and 2 mL of dichloromethane was added. The resulting solution was then filtered through a plug of Celite and evaporated. Crystallization of the crude product from dichloromethane/ether, washing with ether, and drying under vacuum afforded 84 mg (0.09 mmol, 62%) of a product mixture.

(20) Gill, T. P.; Mann, K. R. *Organometallics* **1982**, *1*, 485.
(21) Altomare, A.; Burla, M. C.; Camalli, M.; Cascarano, G.; Giacovazzo, C.; Guagliardi, A.; Moliterni, A. G. G.; Polidori, G.; Spagna, R. *J. Appl. Crystallogr.* **1999**, *32*, 115−119.
(22) Hall, S. R.; Flack, H. D.; Stewart, J. M. *XTAL3.2 User's Manual*; Universities of Western Australia and Maryland, 1992.
(23) Johnson, C. K. *ORTEP II*; Report ORNL-5138; Oak Ridge National Laboratory: Oak Ridge, TN, 1976.
(24) *Chemical Properties* Handbook; McGraw-Hill: New York, 1999 (http://www.Knovel.com).

The second component, which appears in all of these halide extraction experiments, is the known [Ru(η^5-C_5H_5)(BINAP)]-[BF_4][25] (**18**(BF_4)), which results from dissociation of the nitrile and complexation of a naphthyl backbone double bond. This crude product was used for the NMR measurements without further purification. The major product is **9a** (90% by NMR). ^{1}H NMR (300 MHz, CD_2Cl_2): the aromatic protons are found in the range δ 7.85−6.31 (32H, ArH), 4.50 (s, 5H, η^5-C_5H_5), 1.15 (s, 3H, CH_3CN). ^{31}P{^{1}H} NMR (121.4 MHz, CD_2Cl_2): δ 54.5 (d, J_{PP} = 46 Hz), 47.1 (d, J_{PP} = 46 Hz). Minor component [Ru(η^5-C_5H_5)(BINAP)][BF_4], (**18**(BF_4)): ^{1}H NMR (300 MHz, CD_2Cl_2): δ 8.10−8.00 (m, 2H, ArH), 7.90−7.00 (m, 24H, ArH), 6.90−6.70 (m, 1H, ArH), 6.29 (m, 1H, ArH), 6.15−5.90 (m, 4H, ArH), 4.45 (s, 5H, η^5-C_5H_5). ^{31}P{^{1}H} NMR (121.4 MHz, CD_2Cl_2): 74.3 (d, J_{PP} = 44 Hz), 14.2 (d, J_{PP} = 44 Hz).

Synthesis of [Ru(η^5-C_5H_5)(CH_3CN)(BINAP)][CF_3SO_3] (9b). In a typical experiment a Schlenk was loaded with [Ru-(η^5-C_5H_5)(Cl)(BINAP)] (50 mg, 0.06 mmol), $NaSO_3CF_3$ (10 mg, 0.06 mmol), and 2 mL of dry acetonitrile. The solution was then stirred at 80 °C overnight. At the end of the reaction the solvent was evaporated and 2 mL of dichloromethane was added. Subsequent filtration through a plug of Celite, recrystallization from dichloromethane/ether, washing twice with ether, and drying under vacuum afforded 46 mg (0.05 mmol, 83%) of the final product mixture. The mixture could not be further purified and was used as such. Major product (89% by NMR) [Ru(η^5-C_5H_5)(CH_3CN)(BINAP)][CF_3SO_3] (**9b**): ^{1}H NMR (250 MHz, CD_2Cl_2): the aromatic protons are found in the range δ 7.85−6.28 (32H, ArH), 4.48 (s, 5H, η^5-C_5H_5), 1.11 (s, 3H, CH_3CN). ^{31}P{^{1}H} NMR (101.2 MHz, CD_2Cl_2): δ 54.5 (d, J_{PP} = 46 Hz), 47.1 (d, J_{PP} = 46 Hz). One finds ca. 11% of **18**(OTf).

Synthesis of [Ru(η^5-C_5H_5)(CH_3CN)(BINAP)][PF_6] (9c). In a typical experiment a Schlenk was loaded with RuCl(η^5-C_5H_5)(BINAP) (133 mg, 0.16 mmol), $AgPF_6$ (41 mg, 0.16 mmol), and 2 mL of dry acetonitrile. The solution was then stirred overnight in the dark. At the end of the reaction the solvent was evaporated and 2 mL of dichloromethane was added. Subsequent filtration through a plug of Celite, recrystallization from dichloromethane/ether, washing twice with ether, and drying under vacuum afforded 66 mg (0.07 mmol, 44%) of the final product. The major product (90%) is [Ru(η^5-C_5H_5)(CH_3-CN)(BINAP)][PF_6] (**9b**). ^{1}H NMR (250 MHz, CD_2Cl_2): the aromatic protons are found in the range δ 7.85−6.33 (32H, ArH), 4.51 (s, 5H, η^5−C_5H_5), 1.14 (s, 3H, CH_3CN). ^{31}P{^{1}H} NMR (101.2 MHz, CD_2Cl_2): δ 54.5 (d, J_{PP} = 46 Hz), 47.1 (d, J_{PP} = 46 Hz). One finds ca. 10% of **18**(PF_6).

Synthesis of [Ru(η^5-C_5H_5)(CH_3CN)(BINAP)][BArF] (9d). A Schlenk tube was loaded with [RuCl(η^5-C_5H_5)(BINAP)] (50 mg 0.06 mmol), NaBArF (54 mg, 0.06 mmol), and 2 mL of acetonitrile. The solution was then stirred overnight at 80 °C, after which time the solvent was evaporated and 2 mL of dichloromethane was added. The resulting solution was filtered through a plug of Celite and evaporated. The crude product was washed twice with pentane and dried under vacuum to give 49 mg (0.03 mmol, 62%) of the final product [Ru(η^5-C_5H_5)(CH_3CN)(BINAP)][BArF] (**9d**). ^{1}H NMR: (250 MHz, CD_2Cl_2) δ 7.90−6.29 (44H, ArH), 4.47 (s, 5H, η^5-C_5H_5), 1.15 (s, 3H, CH_3CN). ^{31}P{^{1}H} NMR (101.2 MHz, CD_2Cl_2): δ 55.2 (d, J_{PP} = 46 Hz), 47.0 (d, J_{PP} = 46 Hz).

Synthesis of the Acrylonitrile Complexes [Ru(η^5-C_5H_5)-(acrylonitrile)(BIPHOP-F)][Y] and [Ru(η^5-C_9H_7)(acrylo-nitrile)(BIPHOP-F)][Y]: General Procedure. The appropriate complex [Ru(η^5-C_5H_5)(acetone)(BIPHOP-F)][Y] or [Ru-(η^5-C_9H_7)(acetone)(BIPHOP-F)][Y][9] was dissolved in CH_2Cl_2 and degassed by three freeze−pump−thaw cycles. Then acrylonitrile (20 equiv) was added, and the solution was stirred at room temperature for 5 min. After removing volatiles under vacuum, two more cycles of acrylonitrile-addition/stirring/evaporation were performed. Finally, removal of the solvent afforded the product as a yellow powder in quantitative yield. Crystals suitable for X-ray measurements were obtained from CH_2Cl_2/hexane.

[Ru(η^5-C_5H_5)(acrylonitrile)(BIPHOP-F)][BF_4] (*RR*-15a). ^{1}H NMR (300 MHz, $CDCl_3$): δ 7.23−6.91 (m, 6H, ArH), 6.83 (brs, 2H, ArH), 6.64−6.42 (m, 3H, CHOP, ArH), 6.24 (d, J = 18.0 Hz, 1H, CH_2), 6.10 (d, J = 12.0 Hz, 1H, CH_2), 5.75−5.65 (dd, J = 18.0 Hz, J = 12 Hz, 1H, NCCH), 5.07−5.02 (dd, J = 15.0 Hz, J = 8.0 Hz, 1H, CHOP), 5.03 (s, 5H, η^5-C_5H_5). ^{31}P-{^{1}H} NMR (121.5 MHz, $CDCl_3$): δ 129.0 (d, J_{pp} = 65 Hz), 124.0 (d, J_{pp} = 65 Hz). ^{19}F{^{1}H} NMR (282 MHz, $CDCl_3$): δ −142.2 (br, 4F, *o*-C_6F_5), −143.7 (br, 4F, *o*-C_6F_5), −147.0 (m, 2F, *p*-C_6F_5), −147.9 (m, 2F, *p*-C_6F_5), −152.3 (s, BF_4), −158.2 (br, 8F, *m*-C_6F_5). HRMS: calcd for $C_{46}H_{20}O_2NF_{20}P_2Ru$ 1155.972, found 1155.975. $[\alpha]^{20}_D$ +74.54 (CH_2Cl_2, *c* 0.5). CD (CH_2Cl_2, $C = 1 \times 10^{-4}$ M, 20 °C): $\lambda(\Delta\epsilon)$ 353 (+4.21), 286 (−19.38), 250 (−16.49).

[Ru(η^5-C_5H_5)(acrylonitrile)(BIPHOP-F)][BArF] (*RR*-15b). ^{1}H NMR (300 MHz, $CDCl_3$): δ 7.71 (s, 8H, BArF), 7.52 (s, 4H, BArF), 7.16−7.06 (m, 6H, ArH), 6.43 (d, J = 18.0 Hz, 1H, CH_2), 6.30 (d, J = 12.0 Hz, 1H, CH_2), 6.24−5.97 (m, 5H, CHOP, ArH), 5.64 (dd, J = 18.0 Hz, J = 12.0 Hz, 1H, NCCH), 4.94 (br, 1H, CHOP), 4.82 (s, 5H, η^5-C_5H_5). ^{31}P{^{1}H} NMR (121.5 MHz, $CDCl_3$): δ 129.2 (d, J_{pp} = 61 Hz), 124.2 (d, J_{pp} = 61 Hz). ^{19}F{^{1}H} NMR (282 MHz, $CDCl_3$): δ −62.9 (s, CF_3), −140.6 (br, 4F, *o*-C_6F_5), −142.00 (br, 4F, *o*-C_6F_5), −145.2 (m, 2F, *p*-C_6F_5), −146.1 (m, 2F, *p*-C_6F_5), −157.5 (m, 8F, *m*-C_6F_5). HRMS: calcd for $C_{46}H_{20}O_2NF_{20}P_2Ru$ 1155.972, found 1155.973. $[\alpha]^{20}_D$ +80.62 (CH_2Cl_2, *c* 0.5). CD (CH_2Cl_2, $C = 1 \times 10^{-4}$ M, 20 °C): $\lambda(\Delta\epsilon)$ 351 (+5.30), 285 (−26.11), 248 (−20.48).

[Ru(η^5-C_9H_7)(acrylonitrile)(BIPHOP-F)][BF_4] (16a). Yield: 88%. ^{1}H NMR (300 MHz, acetone-d_6): δ 7.66−7.56 (m, 2H, ArH, η^5-C_9H_7), 7.51−7.45 (m, 2H, ArH, η^5-C_9H_7), 6.73−6.64 (m, 2H, ArH, η^5-C_9H_7), 7.36−6.94 (m, 12H, ArH, η^5-C_9H_7, CHOP), 6.60 (dd, J = 18.0 Hz, J = 12.0 Hz, 1H, NCCH), 6.41 (d, J = 12 Hz, 1H, CH_2), 6.37 (d, J = 18.0 Hz, 1H, CH_2), 5.53 (q, J = 9.0 Hz, 1H, CHOP), 5.21 (s, 1H, η^5-C_9H_7), 4.83 (t, J = 9.0 Hz, 1H, η^5-C_9H_7), 4.42 (s, 1H, η^5-C_9H_7). ^{31}P{^{1}H} NMR (121.5 MHz, $CDCl_3$): δ 132.4 (d, J_{pp} = 56 Hz), 127.3 (d, J_{pp} = 56 Hz). ^{19}F{^{1}H} NMR (282 MHz, $CDCl_3$): δ −141.2 (br, 4F, *o*-C_6F_5), −142.0 (br, 4F, *o*-C_6F_5), −145.9 (m, 2F, *p*-C_6F_5), −146.3 (m, 2F, *p*-C_6F_5), −152.0 (s, BF_4), −158.5 (br, 8F, *m*-C_6F_5). HRMS: calcd for $C_{50}H_{22}O_2NF_{20}P_2$ Ru 1205.9877, found 1205.986.

[Ru(η^5-C_9H_7)(acrylonitrile)(BIPHOP-F)][BArF] (16b). Yield: 90%. ^{1}H NMR (300 MHz, acetone-d_6): δ 7.75 (s, 8H, BArF), 7.55 (s, 4H, BArF), 6.73−6.64 (m, 2H, ArH, η^5-C_9H_7), 7.49−7.40 (m, 2H, ArH, η^5-C_9H_7), 7.21−7.14 (m, 3H, ArH, η^5-C_9H_7) 7.08−6.03 (m, 4H, ArH, η^5-C_9H_7), 6.73−6.674 (m, 3H, ArH, η^5−C_9H_7) 7.36−6.94 (m, 12 H, ArH, η^5-C_9H_7), 6.50 (br, 2H), 6.30 (d, J = 18.0 Hz, 1H, CH_2), 6.20 (d, J = 12.0 Hz, 1H, CH_2), 5.60 (dd, J = 18.0 Hz, J = 12.0 Hz, 1H, NCCH), 5.33 (s, 1H), 5.02 (s, 1H, η^5-C_9H_7), 4.94 (t, J = 9.0 Hz, 1H, η^5-C_9H_7), 4.79 (q, J = 6.0 Hz, 1H, CHOP), 4.51 (s, 1H, η^5-C_9H_7). ^{31}P{^{1}H} NMR (121.5 MHz, $CDCl_3$): δ 133.2 (d, J_{pp} = 53 Hz), 128.6 (d, J_{pp} = 53 Hz). ^{19}F{^{1}H} NMR (282 MHz, $CDCl_3$): δ −62.4 (s, CF_3), −139.4 (m, 4F, *o*-C_6F_5), −140.8 (m, 4F, *o*-C_6F_5), −143.5 (m, 2F, *p*-C_6F_5), −144.4 (m, 2F, *p*-C_6F_5), −156.3 (br, 8F, *m*-C_6F_5). HRMS: calcd for $C_{50}H_{22}O_2NF_{20}P_2Ru$ 1205.9877, found 1205.9906.

Synthesis of [Ru(η^5-C_5H_5)(BIPHOP-F)(CH_3CN)][BF_4] (17a). A 10 mM solution (ca. 2 mg in 0.6 mL of CD_2Cl_2) of [Ru(η^5-C_5H_5)(acetone or water)(BIPHOP-F)][Y] (Y = BF_4 or BArF) was placed in an NMR tube. Dry acetonitrile (1 μL) was added, thereby generating the complex quantitatively in situ. The volatile materials were removed, and a fresh equivalent of acetonitrile was added. ^{1}H NMR (400 MHz, CD_2Cl_2): δ 7.20−6.71 (10H, ArH), 5.48 (m, 1H, CH), 4.88 (m, 1H, CH), 4.86 (s, 5H, η^5-C_5H_5), 2.70 (s, 3H, Ru-CH_3CN), 2.06 (s, 3H, free acetone), 1.91 (s, free CH_3CN). ^{31}P{^{1}H} NMR (161.9 MHz, CD_2-

(25) (a) den Reijer, C. J.; Dotta, P.; Pregosin, P. S.; Albinati, A. *Can. J. Chem.* **2001**, *79*, 693. (b) Geldbach, T. J.; Pregosin, P. S. *Eur. J. Inorg. Chem.* **2002**, 1907.

Cl_2): δ 124.8 (d, J_{pp} = 65 Hz), 129.6 (d, J_{pp} = 65 Hz). $^{19}F\{^1H\}$ NMR (376 MHz, CD_2Cl_2): δ −141.2 (br, 4F, *o*-C_6F_5), −142.0 (br, 4F, *o*-C_6F_5), −145.9 (m, 2F, *p*-C_6F_5), −146.3 (m, 2F, *p*-C_6F_5), −152.0 (s, BF_4), −158.5 (br, 8F, *m*-C_6F_5).

Synthesis of the CO Complexes [Ru(η^5-C_5H_5)-(BIPHOP-F)(CO)][Y] (8): General Procedure. The appropriate [(η^5-C_5H_5)Ru(BIPHOP-F)(acetone)][Y] complex was dissolved in CH_2Cl_2 and degassed using three freeze−pump−thaw cycles. One atmosphere of CO was then allowed into the reaction vessel, and the reaction mixture was stirred while bubbling CO through the solution for 15 min. Volatiles were removed under vacuum, yielding the pale yellow carbonyl complexes quantitatively.

[Ru(η^5-C_5H_5)(CO)(BIPHOP-F)][BF_4] (7a). IR (neat, cm^{-1}): 2028 (ν_{CO}). ^1H NMR (300 MHz, acetone-d_6): δ 7.48−7.643 (m, 14H, ArH), 6.21−5.89 (m, 1H, CHOP), 5.82 (s, 5H, η^5-C_5H_5), 5.77 (t, J = 8.0 Hz, 1H, CHOP). $^{31}P\{^1H\}$ NMR (121.5 MHz, $CDCl_3$): δ 128.6 (d, J_{pp} = 46 Hz), 119.9 (d, J_{pp} = 46 Hz). $^{31}P\{^1H\}$ NMR (121.5 MHz, acetone-d_6): δ 127.6 (d, J_{pp} = 45 Hz), 119.6 (d, J_{pp} = 45 Hz). $^{19}F\{^1H\}$ NMR (282 MHz, $CDCl_3$): δ −139.1 (br, 4F, *o*-C_6F_5), −140.0 (br, 4F, *o*-C_6F_5), −142.9 (m, 2F, *p*-C_6F_5), −144.0 (m, 2F, *p*-C_6F_5), −153.3 (s, BF_4), −157.4 (br, 8F, *m*-C_6F_5). $^{19}F\{^1H\}$ NMR (282 MHz, acetone-d_6): δ −144.0 (br, 4F, *o*-C_6F_5), −145.5 (br, 4F, *o*-C_6F_5), −148.0 (m, 2F, *p*-C_6F_5), −148.9 (m, 2F, *p*-C_6F_5), −151.9 (s, BF_4), −160.8 (br, 8F, *m*-C_6F_5). HRMS: calcd for $C_{44}H_{17}O_3F_{20}P_2$ Ru 1130.9404, found 1130.9457.

[Ru(η^5-C_5H_5)(CO)(BIPHOP-F)][BArF] (7b). IR (neat, cm^{-1}): 2033 (ν_{CO}). ^1H NMR (300 MHz, $CDCl_3$): δ 7.75 (s, 8H, BArF), 7.53 (s, 4H, BArF), 7.26−7.19 (m, 4H, ArH), 7.17 (br, 2H, ArH), 6.93 (d, J = 7.0 Hz, 2H, ArH), 6.66 (br, 2H, ArH), 5.28 (q, J = 8.0 Hz,1H, CHOP), 5.19 (s, 5H, η^5-C_5H_5), 4.94 (t, J = 8.0 Hz 1H, CHOP). ^1H NMR (300 MHz, acetone-d_6): δ 7.79 (s, 8H, BArF), 7.67 (s, 4H, BArF), 7.27−7.18 (m, 6H, ArH), 7.09 (br, 4H, ArH), 5.90−5.87 (m, 1H, CHOP), 5.83 (s, 5H, η^5-C_5H_5), 5.76 (t, J = 8.0 Hz 1H, CHOP). $^{31}P\{^1H\}$ NMR (121.5 MHz, $CDCl_3$): δ 127.6 (d, J_{pp} = 42 Hz), 117.7 (d, J_{pp} = 42 Hz). ^{31}P NMR (121.5 MHz, acetone-d_6): δ 127.6 (d, J_{pp} = 51 Hz), 119.4 (d, J_{pp} = 51 Hz). $^{19}F\{^1H\}$ NMR (282 MHz, $CDCl_3$): δ −62.6 (s, CF_3), −136.6 (br, 4F, *o*-C_6F_5), −137.9 (br, 4F, *o*-C_6F_5), −141.0 (m, 2F, *p*-C_6F_5), −142.3 (m, 2F, *p*-C_6F_5), −155.1 (m, 8F, *m*-C_6F_5). ^{19}F NMR (282 MHz, acetone-d_6): δ −63.2 (s, CF_3), −144.0 (br, 4F, *o*-C_6F_5), −145.4 (br, 4F, *o*-C_6F_5), −148.0 (m, 2F, *p*-C_6F_5), −149.0 (m, 2F, *p*-C_6F_5), −159.6 (m, 8F, *m*-C_6F_5). HRMS: calcd for $C_{44}H_{17}O_3F_{20}P_2$ Ru 1130.9404, found 1130.9398.

Acknowledgment. E.P.K. thanks G. Hopfgartner for the TOF-MS measurements. Special thanks are due to H. Rüegger and M. Valentini for both experimental assistance and timely advice. E.P.K. and P.S.P. thank the Swiss National Science Foundation for financial support. P.S.P. thanks the BBW and the ETH Zürich for financial support and Johnson Matthey for the loan of precious metal compounds.

Supporting Information Available: X-ray crystallographic data, including cif files, and tables of bond lengths and angles for compounds *RR*-**15a** and *RR*-**15b**. This material is available free of charge via the Internet at http://pubs.acs.org.

OM049559O